

Journal of Materials Chemistry C

Accepted Manuscript



This article can be cited before page numbers have been issued, to do this please use: S. Pagidi, N. Kalluvettukuzhy K and P. Thilagar, *J. Mater. Chem. C*, 2017, DOI: 10.1039/C7TC01676J.



This is an Accepted Manuscript, which has been through the Royal Society of Chemistry peer review process and has been accepted for publication.

Accepted Manuscripts are published online shortly after acceptance, before technical editing, formatting and proof reading. Using this free service, authors can make their results available to the community, in citable form, before we publish the edited article. We will replace this Accepted Manuscript with the edited and formatted Advance Article as soon as it is available.

You can find more information about Accepted Manuscripts in the [author guidelines](#).

Please note that technical editing may introduce minor changes to the text and/or graphics, which may alter content. The journal's standard [Terms & Conditions](#) and the ethical guidelines, outlined in our [author and reviewer resource centre](#), still apply. In no event shall the Royal Society of Chemistry be held responsible for any errors or omissions in this Accepted Manuscript or any consequences arising from the use of any information it contains.

H-bond Assisted Mechanoluminescence of Borylated Aryl Amines: Tunable Emission and Polymorphism

Pagidi Sudhakar, Kalluvettukuzhy K Neena and Pakkirisamy Thilagar*

Received 00th January 20xx,
Accepted 00th January 20xx

DOI: 10.1039/x0xx00000x

www.rsc.org/

Design, synthesis and structural characterization of borylated aryl amines, Mes_2BAr {Ar = $\text{C}_6(\text{CH}_3)_4\text{NR}_2$ (**1**, **4**); $\text{C}_6\text{H}_4\text{NR}_2$ (**2**, **5**); $\text{C}_6\text{H}_4(\text{NR}_2)_2$ (**3**, **6**); R=H or CH_3 } were reported. The intriguing optical signatures undoubtedly revealed their donor-acceptor features and bright tunable solid state emission is readily realized. The solid state luminescence characteristics of **1** and **3** were sensitive to mechanical stress with distinguishable emission color changes. Multiple strong intermolecular hydrogen bonds (N-H \cdots N and N-H \cdots π) accompanied by subtle conformational changes play a significant role in the piezochromic response. PXRD and FT-IR spectroscopic studies and insensitivity of substituted derivatives to mechanical stress support the above inference. Interestingly, compound **3** crystallized in two different polymorphic forms **3BP** and **3GP**, which showed distinct luminescence, i.e., green and blue color under UV light. Such changes are due to their distinct hydrogen-bond network assembly in the solid state. Quantum mechanical calculations were performed in order to corroborate the optical properties.

Introduction

Recently, a lot of research effort has been devoted to the development of smart materials which change their luminescence color upon exposure to an external stimuli such as pressure, mechanical force, temperature and chemical vapours.^{1,2} Smart materials which change their emission characteristics under mechanical force like shearing, grinding, tension or hydrostatic pressure are called mechanochromic luminescent materials.³⁻⁵ Last decade has witnessed a tremendous progress in the field of mechanofluorochromic materials.³⁻¹¹ Tuning and switching the luminescence color of organic materials by regulating the mode of molecular packing or by changing the molecular conformations, instead of alteration of the chemical structure is an attractive strategy for both fundamental research and practical applications.⁵ Recent studies on mechanofluorochromic materials have revealed that the color changes in these materials are mainly due to changes in their solid state packing, which are largely driven by intermolecular interactions.^{6,7}

Despite the outburst developments happened in the field of H-hydrogen bonding, there are only very few reports on hydrogen bond assisted piezochromic materials.⁸ Yamaguchi and co-workers elegantly demonstrated H-bond directed distinct luminescent responses of 2,3,4,5-tetra(2-

thiazolyl)thiophene towards anisotropic grinding and isotropic compression.^{8b} Araki and co-workers investigated H-bond assisted mechanochromic luminescent response of pyrene assemblies with amide substituents as the H-bonding sites.^{8a,b} Most of reported hydrogen bond based materials/liquid crystals consist of planar aromatic skeletons and hydrogen bonding sites, and thus $\pi\cdots\pi$ stacking and hydrogen bonding play a synergistic role for their switchable color changes when pressure is applied.^{8,9} However, planar aromatic skeleton may reduce the fluorescence in the solid state due to undesirable interactions.¹⁰ In order to access highly fluorescent mechanochromic materials, bulky groups or aggregation induced emissive fluorogens (AIEgens) need to be incorporated in the smart materials. Several designed mechanochromic molecules are based on existing AIEgens.¹¹ Considering the demand of smart materials in the global market, there is an urgent need for developing novel mechanochromic materials with strong solid state fluorescence and good color contrast.

In recent years, triarylborane (TAB) based systems have attracted considerable attention because of their potential applications in OLEDs, sensors etc.¹²⁻¹⁵ If a suitable donor is attached to electron deficient triarylboranes, bright solid state emission is achieved owing to the propeller geometry of TAB and intramolecular charge transfer (ICT) features between donor and acceptor. Although, numerous TAB based D-A systems are well documented in the literature,¹²⁻¹⁵ the mechanochromic luminescent characteristic of these systems has not been realized in spite of the importance of such materials in modern technology.

Recent work from our laboratory showed that subtle conformational changes in TAB based D-A structures have

Department of Inorganic and Physical Chemistry, Indian Institute of Science, Bangalore, 560012, India. Tel: +91-080-2293-3353, Fax: +91-23601552
Email: thilagar@ipc.iisc.ernet.in

Electronic Supplementary Information (ESI) available: [Synthetic procedures, NMR and HRMS spectral data, photophysical properties, DFT and TD-DFT results, single crystal X-ray analysis data, PXRD and IR data. CCDC No. 1530085-1530088, 1407288, 947986]. See DOI: 10.1039/x0xx00000x

tremendous impact on their optical properties.¹⁵ We envisaged that the introduction of propeller shaped TAB and hydrogen-bonding sites (-NH₂) within the same molecular framework could be an effective strategy for the development of strongly fluorescent smart materials. Herein we report that the designed molecules meet our anticipation that gentle grinding of **1** and **3** showed an altered emission (chart 1). To demonstrate that hydrogen bonding does play a crucial for the mechanofluorochromism, hydrogen atoms on the -NH₂ moiety were replaced with methyl groups to eliminate the formation of hydrogen bonds and the corresponding methylated derivatives did not show any response to external stress. We also found that compound **3** forms polymorphs with distinct optical features.

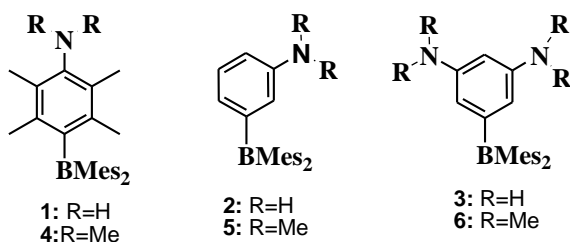


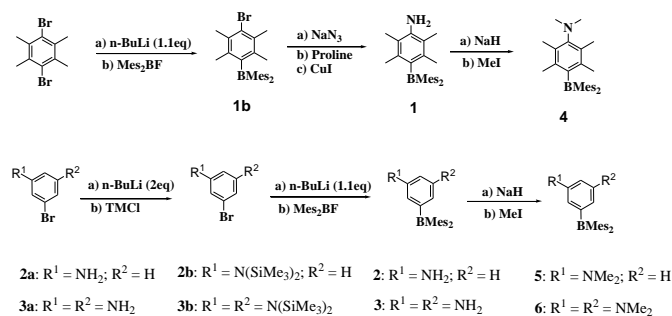
Chart 1. Chemical structures of borylated aryl amines 1-6.

Results and discussions

Synthesis and characterization

Unsubstituted borylated aryl amines can be conveniently prepared by the Williams¹⁶ and Asher's¹⁷ method. Recently, Thilagar *et al.*^{15a} developed a facile synthetic route which has several advantages such as a less reaction time and excludes the use of heavy metal (Pd). A similar procedure has been followed for the synthesis of **2** and **3**, in 90% and 80% yield, respectively (Scheme S1). First lithiation of appropriate bromoanilines using required amount of *n*-BuLi (two equivalents for **2a** and four equivalents for **3a**) generated anion on nitrogen centre(s), which was trapped with trimethylsilyl chloride to yield the corresponding *N*-bistrimethylsilyl protected bromoanilines **2b** and **3b**. Subsequently, addition of one equivalent of *n*-BuLi replaces bromine and generates a carbanion, which was then quenched with dimethylfluoroborane followed by methanolysis to obtain the respective borylated aryl amines **2** and **3**. Synthesis of **1** involves heating a mixture of (4-bromo-2,3,5,6-tetramethylphenyl)dimesitylborane with L-proline, sodium azide and copper(I) iodide in DMSO at 100 °C (Scheme 1). Compounds **4**, **5** and **6** were synthesized in moderate yields by methylation of **1**, **2** and **3** using sodium hydride and methyl iodide. The synthesis of compound **2** was reported by Wang and co-workers using Williams Method,^{16f} but its optical properties have not been investigated. Hence, we prepared **2** for comparative studies to get an insight into the optical properties of other compounds **1**, **3**, **4**, **5** and **6**. Compounds **1-6** are quite stable under ambient conditions. All the

compounds were characterized by multi-nuclear NMR (¹H and ¹³C) and high resolution mass spectrometry (HRMS).



Scheme 1. Synthesis of compounds 1-6

Optical Properties

Hexane solutions (10 μM) of compounds **1-6** showed two major absorption features in the range 280-450 nm; in contrast, compound **4** displayed a single absorption band (280-420 nm, Figure 1). In order to rationalise the absorption features, the UV-Vis absorption profiles of all the compounds were recorded in solvents of different polarity. Upon increasing the solvent polarity, the lower energy band of **1**, **2**, **3**, **5** and **6** was bathochromically shifted, while the higher energy band was unaffected (Figure S25 and Table S1). From these results, we can infer that the lower energy band arises from amine to boron intramolecular charge transfer and the higher energy band is from boron bound aryl centred π-π* transitions. However, the absorption spectra of **4** did not show any significant changes in solvents of varying polarity. Absence of ICT band in **4** can be attributed to the poor electronic communication between boron and nitrogen; presumably due to the presence methyl groups on the nitrogen centre twisted the duryl (spacer) unit significantly.

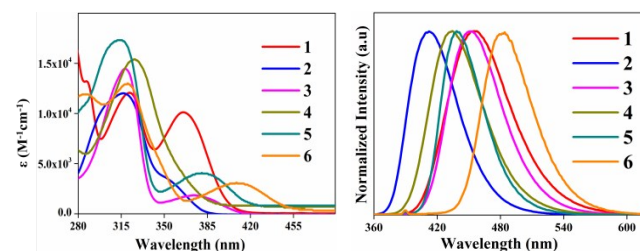


Figure 1. Absorption (left) and emission (right) spectra of **1-6** in hexane solutions (Conc. 10 μM, λ_{ex} = 350 nm).

To gain an in-depth understanding of the electronic structure of **1-6** geometry optimizations were carried out with density functional theory using B3LYP hybrid functional and 6-31G (d) basis set.²⁰ The geometric parameters of energy minimized structures (Figure S28) of the compounds closely resembled the data from X-ray crystal structures (Table S4). The molecular orbital coefficients of HOMO in **1-6** are localised on arylamine unit. The LUMO of **1-6** is localised on the triarylborene moiety (Figure 2). The non-crossing HOMO and LUMO molecular orbitals (MOs) of **1-6** support the presence of ICT from donor amine to acceptor boryl unit. Further, the

calculated HOMO-LUMO gap in **1-6** follows the trend experimentally observed in UV-Vis spectral studies (Figure 1). Compounds **1-6** showed an excitation wavelength independent broad emission around 455, 412, 451, 435, 438 and 484 nm respectively in hexane solutions (Figure 1). Unlike the absorption spectra, fluorescence spectra of these compounds are remarkable and showed significant solvatochromism with higher Stokes shift (Figure S26 and Table S1), which are characteristic of boron based D-A system reported elsewhere.^{13,14} Dipole moment of the fluorescent state of the compounds were calculated using Lippert-Mataga equation,¹⁹ i.e., from the Stokes shift and the solvent orientation parameter. The estimated excited state dipole moments of **1, 2, 3, 4, 5** and **6** are 13.34, 16.83, 11.96, 14.39, 13.02, and 11.20 respectively, undoubtedly support the charge-transfer character of the excited state (Table S2). Fluorescence life times were recorded in hexane, dichloromethane and DMSO. The decay data could be fitted into a double exponential function (Table S3). Increase in longer lifetime species in polar dichloromethane or DMSO compared to non-polar hexane clearly indicates that the longer life time species originated from highly polarized ICT/TICT (twisted intramolecular charge transfer) state and shorter life time species arose from the locally excited state.

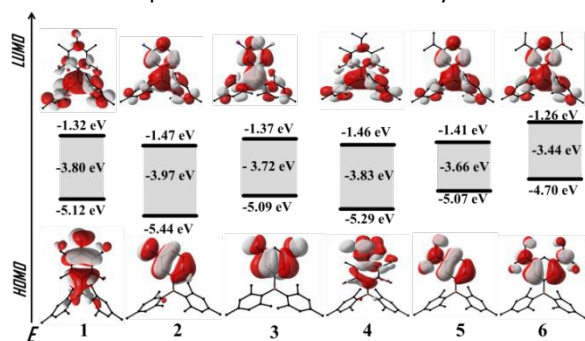


Figure 2. Calculated frontier molecular orbitals and the orbital energies (eV) of **1-6** (energy levels are not to scale). (Atom colour codes: B: orange, N: blue, C: black, hydrogen atoms are omitted for clarity).

In the solid state, compounds **1-6** showed unstructured emission peaked at ~ 446 , ~ 433 , ~ 469 , ~ 437 , ~ 452 and ~ 504 nm respectively upon excitation at 350 nm (Figure 3). Compounds **1-6** followed the similar trend as observed in solution state. The absolute fluorescence quantum yields determined for pristine solid powders of **1, 2, 3, 4, 5** and **6** are 10.7, 22.2, 40.3, 29.9, 31.0 and 38.6 % respectively. The fluorescence decay rate constants (k_r) and non-radiative decay rate constants (k_{nr}) are calculated by using the average fluorescence lifetimes and quantum yields. The higher solid state quantum yields observed for **3** and **6** are due to relatively small k_{nr} values resulting in suppression of non-radiative relaxation. (Table S6).

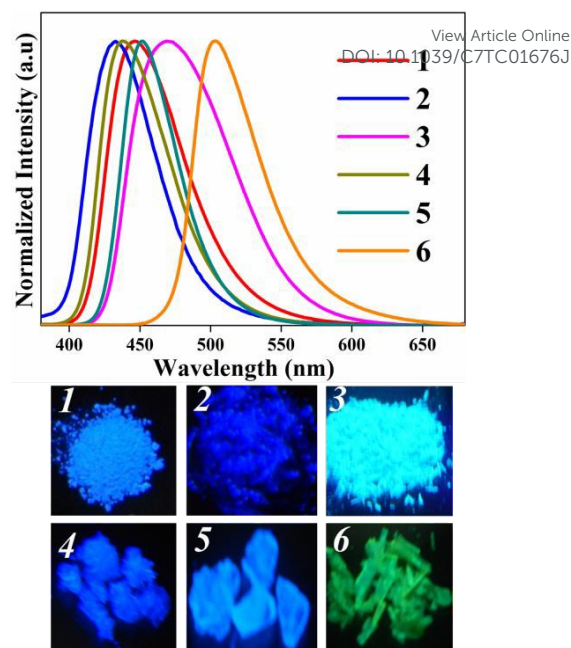


Figure 3. Solid state emission spectra of **1-6** ($\lambda_{ex} = 350$ nm). Images of compound under UV light illumination (bottom, $\lambda_{ex} = 365$ nm).

Structural Characterization-Polymorphism

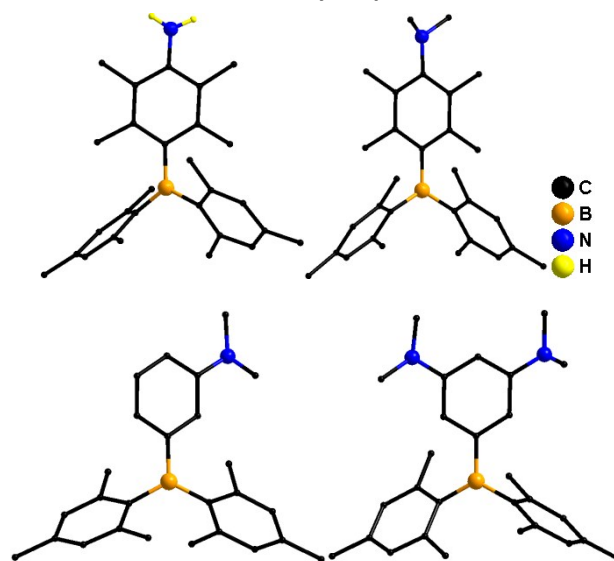


Figure 4. Molecular structures of **1** (top left), **4** (top right), **5** (bottom left), and **6** (bottom right), (H atoms except those coordinated to N atom of **1** are omitted for clarity).

To gain a molecular level understanding of the luminescence characteristics of compounds **1-6**, crystallization of these compounds were carried out. Single crystals suitable for X-ray diffraction were obtained by slow evaporation of **1** from solutions of EtOAc, **4, 5** and **6** from DCM solutions (Figure 4, Table S9). Interestingly, compound **3** forms polymorphs, by slow evaporation of hexane (**3GP**) and DCM (**3BP**) solutions, respectively (Figure 6, 7 and Table S7). The boron atom in compounds **1, 3BP** and **3GP, 4, 5** and **6** has a trigonal planar configuration with the sum of angles around boron being 360° . However, the nitrogen centre(s) adopt slightly pyramidal

geometry; the sums of angles around N add up to $\sim 342\text{--}350^\circ$. In the solid state, compound **1** showed unique N–H... π interactions (π system of duryl moiety) and forms a one dimensional zig-zag chain with a N–H... π distance of 2.49 Å (Figure 5). The N–H... π interaction observed in **1** (2.49 Å) is quite stronger compared to recently reported 4-(dimesitylboryl)aniline (3.02 Å), 4-(dimesitylboryl)-3,5-dimethylaniline (4.08 Å).^{15a}

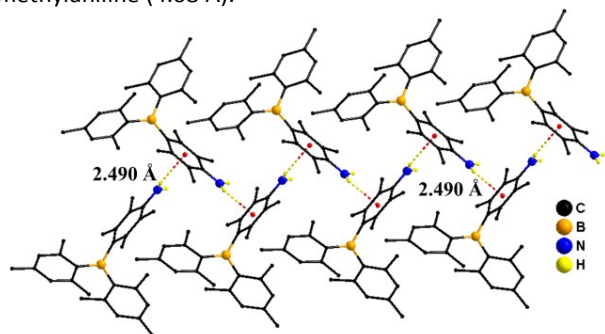


Figure 5. Intermolecular (N–H... π) interaction in the molecular structure of **1** (H atoms except those coordinated to N atom are omitted for clarity).

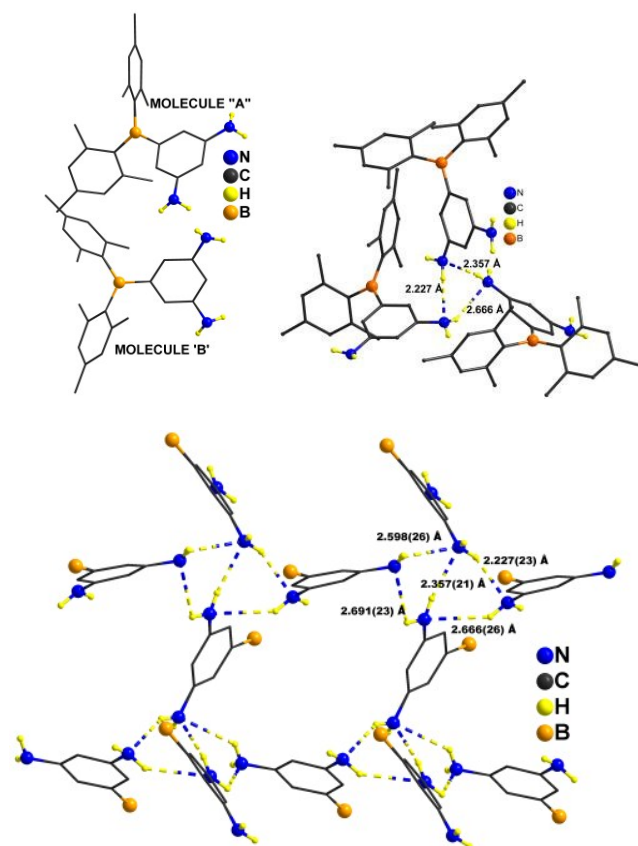


Figure 6. Asymmetric unit content (top left) of **3BP**. Representation of formation of intermolecular trimer in solid state of **3BP** (top right). Representation of the intermolecular N–H...N interactions between the neighbouring trimers in **3BP** (bottom). All the hydrogen atoms (except –NH₂ unit) are omitted for clarity.

Interestingly, the polymorphs of **3** showed different emission colours under UV light illumination. **3BP** crystal showed blue colour emission (~ 450 nm) while **3GP** crystal showed green colour (~ 505 nm) emission (Figure 8). Careful examination of

the crystal data revealed that **3BP** crystallized in monoclinic crystal lattice in $P2_1/c$ space group, while **3GP** crystallized in triclinic ($P-1$) crystal lattice. Two crystallographically distinct molecules were present in the asymmetric units of **3BP** (Figure 6, left) and **3GP** (Figure 7, left); these are labelled as molecule A and molecule B respectively and the metric parameters for A and B differ significantly (Table S8).

To understand the distinct emission characteristics of the polymorphs **3BP** and **3GP**, their solid state packing in the crystal lattice was examined. Both **3BP** and **3GP** polymorphs form strong intermolecular N–H...N and N–H... π interactions at several positions. Three neighboring molecules of **3BP** form an intermolecular trimer via N–H...N interactions (Figure 6, middle). One of the two –NH₂ groups of diaminophenyl unit is involved in the formation of intermolecular trimer. The second NH₂ group connects the neighbouring trimers via intermolecular N–H...N interactions and generates 3D supramolecular network structure (Figure 6, right). In case of **3GP**, the intermolecular N–H...N interaction between four of the adjacent molecules generate a tetramer (Figure 6, middle). Further intermolecular N–H...N interaction between the neighbouring tetramers generated 3D supramolecular structure (Figure 7, right). The hydrogen bonds play an important role in fixing the orientation of the donor aniline and acceptor boryl units. The dihedral angle between the BC2 (mesityl carbon) plane and donor aniline in **3BP** and **3GP** were found to be $\sim 38^\circ$ and $\sim 22^\circ$ respectively. The smaller dihedral angle in **3GP** indicates that the donor (aniline) and acceptor (boryl) interactions in **3GP** is stronger than in **3BP**, in support of the red shifted emission of **3GP** compared to **3BP**.

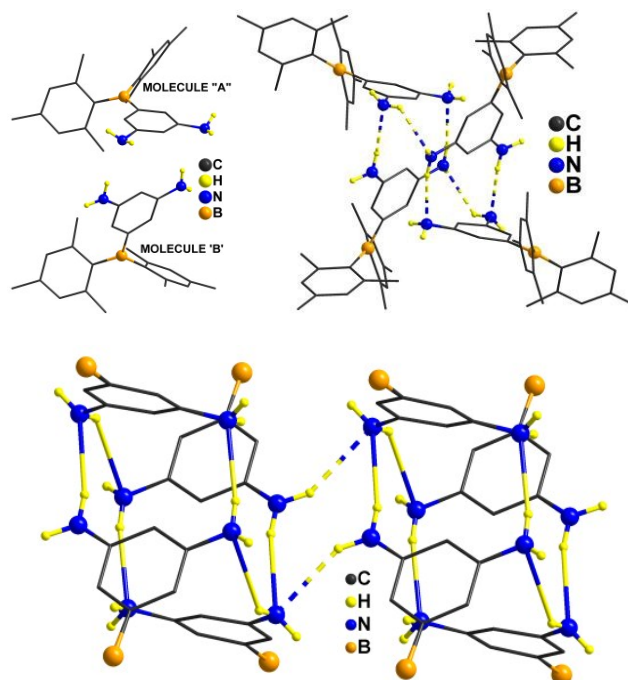


Figure 7. Asymmetric unit content (top left) of **3GP**. Representation of formation of intermolecular tetramer in solid state of **3GP** (top right). Representation of the intermolecular N–H...N interactions between the neighbouring tetramers in **3GP** (bottom). All the hydrogen atoms (except –NH₂ unit) are omitted for clarity.

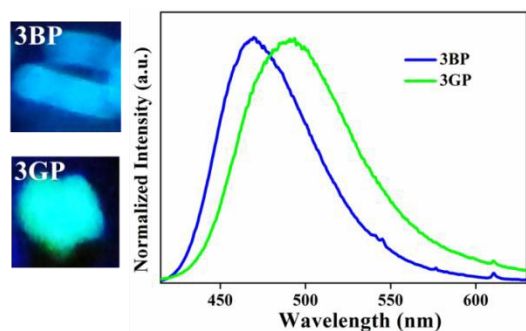


Figure 8. Luminescence spectra of polymorphs **3BP** and **3GP** of compound **3** (right, $\lambda_{\text{ex}} = 350$ nm). Images of single crystals under UV light illumination (left, $\lambda_{\text{ex}} = 365$ nm).

Mechanochromism

The bright solid state luminescence characteristics of **1-6** prompted us to study their solid state PL features under mechanical force. Compounds **1** and **3** only showed altered emission upon mechanical grinding (Figure 9). The emission features of ground samples of **1** and **3** were significantly red shifted from 445 to 465 nm (blue to cyan blue) and 468 to 493 nm (cyan blue to green) respectively. The energy difference in the bathochromic shift sums to 966 and 1083 cm^{-1} . The ground form of **1** and **3** reverted back to original colour by heating at

100 °C for about 30 min. It has been found that the ground form of **1** and **3** showed a higher average excited state life time compared to the pristine sample (Table S11). The absolute fluorescence quantum yields of **1G** and **3G** are 12.2 and 36.5 % respectively. These values indicate that fluorescence quantum yield of ground samples **1G** and **3G** are comparable to the pristine samples of **1** and **3**, respectively. This result is noteworthy in the field of smart materials; only a few materials have been reported to show higher fluorescence quantum yield for unground sample than the ground sample.¹⁸ The pristine and ground samples of **1** and **3** were examined by FT-IR spectroscopy (Figure S30). The pristine sample of **1** showed the NH stretching vibrations around 3383 cm^{-1} and 3476 cm^{-1} , while the ground form (**1G**) displayed peaks at 3401 cm^{-1} and 3482 cm^{-1} . In case of **3**, the peaks corresponding to N-H stretching were observed around 3383 cm^{-1} and 3476 cm^{-1} for pristine form, and 3401 cm^{-1} and 3482 cm^{-1} are for the ground form (**3G**). From these data, the ground forms of **1** and **3** have shown slightly higher N-H stretching vibrations compared to respective pristine forms clearly indicating that the hydrogen bonds were weakened; that could be due to partial perturbation from the ordered structure upon mechanical force.

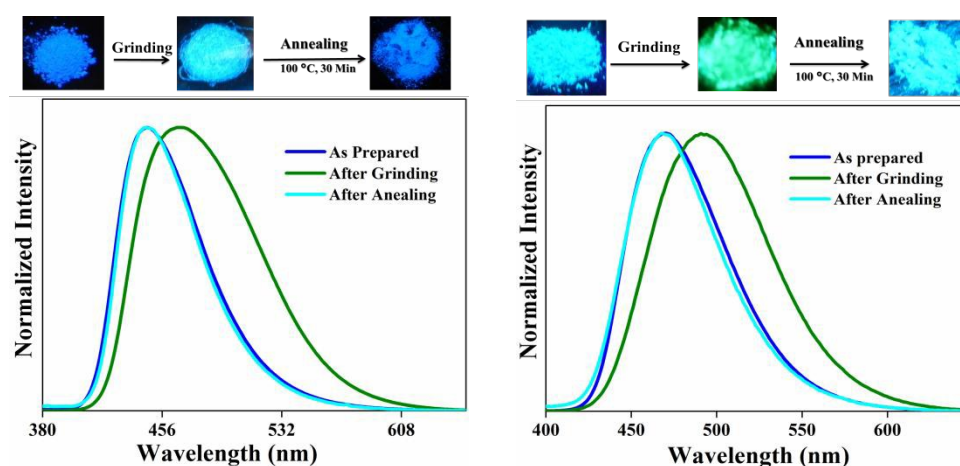


Figure 9. Solid state emission spectra of different samples of **1** (left) and **3** (right) obtained after mechanical grinding ($\lambda_{\text{ex}} = 350$ nm). Images of compounds **1** and **3** under UV-light illumination ($\lambda_{\text{ex}} = 365$ nm).

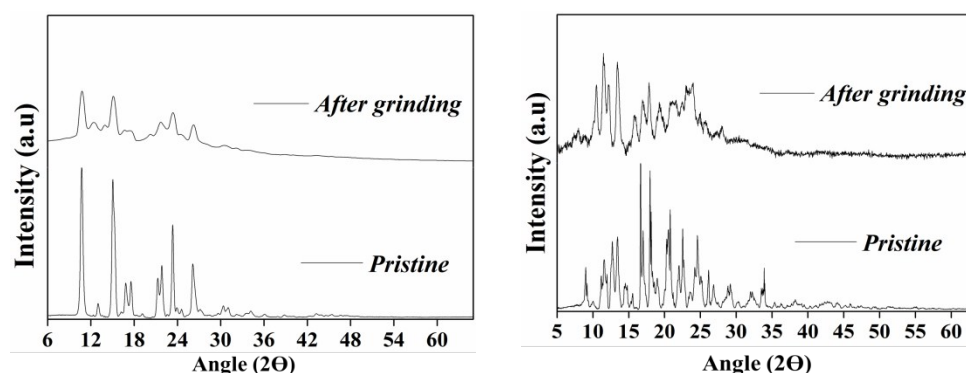


Figure 10. PXRD pattern of different samples of **1** (left) and **3** (right) obtained after mechanical grinding.

ARTICLE

The strong H-bonding interactions observed in the solid states were disturbed by mechanical force and affected the electronic energy levels of the compound. The above inference was further validated by the insensitivity of corresponding methylated derivatives **4** and **6** towards mechanical stress. Compounds **4**, **5** and **6** showed only weak Van der Waals interactions in the solid state (Figure S29). We also checked the luminescence characteristics of previously reported 4-(dimesitylboryl)aniline and 4-(dimesitylboryl)-3,5-dimethylaniline under mechanical pressure and found that those are insensitive despite having H-bonding interactions in the solid state. The possible reason may be the strength of hydrogen bond in above mentioned borylanilines relative to **1** and **3**.^{15a} Evidently, the changes in intermolecular interactions and conformational planarization of **1** and **3** by applied force can permit a more in-plane arrangement of donor and acceptor units and possibly better intermolecular charge transfer interactions, leading to a bathochromic shift in luminescence.

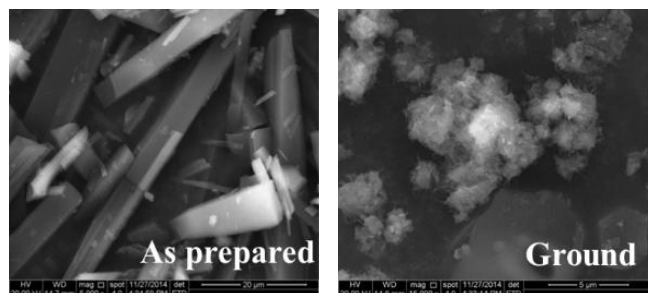


Figure 11. Scanning Electron Microscope (SEM) images of as prepared (left) and ground (right) samples of **3**.

To get further insight into the mechanofluorochromic characteristics of **1** and **3** in the solid state, powder X-ray diffraction (PXRD) analysis were carried out for different samples of **1** and **3** obtained after mechanical treatment (Figure 10). The PXRD pattern of pristine samples of **1** and **3** exhibit sharp and intense reflection peaks indicative of crystalline nature of these compounds. A visible change is noticed in the PXRD pattern of the ground samples of **1** and **3**. The greater full width at half maximum (FWHM) and change in the intensities of the ground samples compared to the pristine ones point to possible deformation of the ordered structures. In order to understand the morphological changes of compounds taking place upon mechanical grinding, scanning electron microscopic (SEM) images of pristine and ground samples were recorded; unfortunately we could not get the SEM images for **1** due to charging. The SEM images of **3** showed noticeable changes in the morphology upon grinding.

Highly ordered crystalline aggregates were observed in the morphological pattern of pristine sample whereas the bigger crystals of **3** were broken into highly disordered aggregates, upon grinding (Figure 11).

Conclusion

A series of borylated aryl amines were conveniently synthesised and structurally characterised. The optical data clearly demonstrated that the ICT can be controlled by steric and electronic factors. Compounds **1** and **3** displayed an altered emission in response to the external stress and controlled experiments demonstrated that non-covalent intermolecular hydrogen bonds (N-H...N and N-H... π) played a pivotal role for the mechanoluminescent response. Substituted amine derivatives (**4**, **5** and **6**) further validated the above inference. Compound **3** crystallized in the two different polymorphic forms which exhibited different emission characteristics due to their distinct supramolecular interactions in the solid state. Owing to strong solid emission and stimuli responsive luminescence these molecules may find applications in smart materials and optoelectronic devices.

Experimental Section

Methods and equipment

All the precursors were purchased from commercial suppliers (Sigma-Aldrich, USA; Merck, Germany; SDFCL, India), and used as received, unless otherwise mentioned. All reactions were carried out under argon atmosphere using standard schlenck-line techniques. THF was dried over sodium and distilled out under argon atmosphere. DCM and chloroform were dried using CaH₂ and stored over 4Å molecular sieves. DMSO was distilled and stored over 4Å molecular sieves. ¹H and ¹³C NMR spectra were recorded at 25 °C on a Bruker Avance 400 MHz NMR Spectrometer operating at a frequency of 400 MHz for ¹H and 100 MHz for ¹³C. ¹H NMR spectra were referenced to TMS (0.00 ppm) as an internal standard. Chemical shift multiplicities are reported as singlet (s), doublet (d), triplet (t), quartet (q), and multiplet (m). ¹³C resonances were referenced to the CDCl₃ signal at ~77.6 ppm. High resolution mass spectra (HRMS) were recorded on a Micromass Q-ToF High Resolution Mass Spectrometer by electrospray ionization (ESI) method. Melting points of the compounds were measured on a calibrated melting point apparatus (Analab), μ Thermocal10. Electronic absorption spectra and fluorescence emission spectra were recorded on a Perkin Elmer LAMBDA 750 UV/visible spectrophotometer and Horiba JOBIN YVON

Fluoromax-4 spectrometer, respectively. Solutions of all the compounds for spectral measurements were prepared using spectrophotometric grade solvents, microbalance (± 0.1 mg precision) and standard volumetric glass wares. Quartz cuvettes with sealing screw caps were used for the solution state spectral measurements. Single-crystal X-ray diffraction studies were carried out with a Bruker SMART APEX diffractometer equipped with 3-axis goniometer. The data were integrated using SAINT, and an empirical absorption correction was applied with SADABS. The structures were solved by direct methods and refined by full matrix least-squares on F^2 using SHELXTL software.²⁰ All the non-hydrogen atoms were refined with anisotropic displacement parameters, while the hydrogen atoms were refined isotropically on the positions calculated using a riding model. Theoretical calculations were performed using the *Gaussian 09* suite of quantum mechanical calculations. The hybrid Becke 3-Lee-Yang-Parr (B3LYP) exchange correlation functional was employed to predict the minimum energy molecular geometries of the compounds. Geometries were fully optimized in the gas phase at the B3LYP level of theory by using the 6-31G(d) basis set for all the atoms. Frequency calculations were performed on each optimized structure using the same basis set to ensure that it was a minimum on the potential energy surface.²¹ Powder X-ray diffraction patterns of compounds were collected from a XD-D1 Shimadzu X-ray diffractometer. SEM micrographs were collected on a field emission scanning electron microscopy (FESEM, FEI Inspect F50), energy dispersive X-ray spectroscopy (EDS, Oxford instrument) attached with FESEM. Solid samples were loaded on carbon tape prior to measurements.

Synthesis

4-(Dimesitylboryl)-2,3,5,6-tetramethylaniline (1): An oven dried two neck round bottom flask was equipped with reflux condenser connected to Schlenk line and another neck with glass stopper. The reaction flask was evacuated and then refilled with argon. The flask was charged with proline (225 mg, 1.50 mmol), sodium azide (150 mg, 2.50 mmol), CuI (220 mg, 1.15 mmol) and (4-bromo-2,3,5,6-tetramethylphenyl)dimesitylborene (250 mg, 0.38 mmol) and then degassed dry DMSO (15 mL) was added. The reaction mixture was slowly warmed to 100 °C (procedure is not recommended for higher scales). During the course of the reaction, the solution turned from colorless to dark green color. After consumption of the starting material (confirmed by TLC), the mixture was filtered through celite and compound was purified by column chromatography over silica-gel, eluting with hexane-ethyl acetate (1:1), gave the pale yellow color solid. Yield: 80%. M.P.: ~ 183 -185 °C. ^1H NMR (400 MHz CDCl_3 , 25 °C): δ (ppm) 6.71 (s, 4H), 3.70 (s, 2H), 2.25 (s, 6H), 2.03 (s, 6H), 1.97 (s, 6H), 1.91 (s, 6H); ^{13}C NMR (100 MHz, CDCl_3 , 25 °C): δ (ppm) 145.7, 143.6, 140.7, 140.7, 139.5, 138.6, 136.5, 128.7, 128.6, 117.7, 23.1, 23.0, 21.3, 20.4, 13.2. ^{11}B NMR (376.5 MHz, CDCl_3 , 25 °C): δ (ppm) 75.6. ESI-MS (positive ion mode): Mcalc. for $\text{C}_{28}\text{H}_{36}\text{BN}$ = 398.3019 Da; found: 398.3315 Da $[\text{M}+\text{H}]^+$.

3-(Dimesitylboryl)aniline (2): Step1:- To a solution of 2-bromoaniline (2 g, 11.62 mmol) in THF (50 mL) at -78 °C was added drop wise *n*-BuLi (14.50 mL of a 1.6 M solution in hexanes, 23.25 mmol), and the reaction mixture was stirred for 1 h at the same temperature. Trimethylsilyl chloride (2.90 g, 26.75 mmol) was added, and the reaction mixture was warmed to room temperature and stirred for 6 h. Volatiles were removed in vacuum, and the product (N-(3-bromophenyl)-1,1,1-trimethyl-N-(trimethylsilyl)silanamine) was distilled out (~ 120 °C) under reduced pressure. Yield: 90%. ^1H NMR (400 MHz, CDCl_3 , 25 °C): δ (ppm) 7.25 (s, 1H), 7.14-7.12 (m, 1H), 7.10 (s, 1H), 6.89 (d, $J = 7.6$ Hz, 1H), 0.14 (s, 18H). Step2:- To a solution of N-(3-bromophenyl)-1,1,1-trimethyl-N-(trimethylsilyl)silanamine (2.0 g, 6.40 mmol) in THF (50 mL) at -78 °C was added dropwise *n*-BuLi (4.40 mL of a 1.6 M solution in hexanes, 7 mmol), and the reaction mixture was stirred for 1 h. Mes_2BF (2 g, 7.20 mmol) in THF (10 mL) was added, and the reaction mixture was warmed to room temperature over 12 h. The solvent was evaporated, and the crude residue was dissolved in methanol and refluxed for 6 h. The reaction mixture was cooled to room temperature and extracted using ethyl acetate. The combined extracts were stored over anhydrous Na_2SO_4 , and the solvent was removed under reduced pressure. The crude product was purified by a column chromatography over neutral alumina using a mixture of petroleum ether and ethyl acetate (95:5 ratios) as eluent to obtain the title compound as an off-white solid. Yield: 90%. M.P.: ~ 178 -180 °C. ^1H NMR (400 MHz, CDCl_3 , 25 °C): δ (ppm) 7.17 (t, $J = 8$ Hz, 1H), 6.96 (d, $J = 6.8$ Hz, 1H), 6.86 (d, $J = 6.8$ Hz, 1H), 6.82 (s, 4H), 6.81 (s, 1H), 3.59 (s, 2H), 2.34 (s, 6H), 2.05 (s, 12H); ^{13}C NMR (100 MHz, CDCl_3 , 25 °C): δ (ppm) 146.4, 142.4, 141.3, 139.0, 129.3, 128.5, 127.3, 122.6, 119.2, 23.8, 21.7. ^{11}B NMR (376.5 MHz, CDCl_3 , 25 °C): δ (ppm) 74.2. ESI-MS (positive ion mode): Mcalc. for $\text{C}_{24}\text{H}_{28}\text{BN}$ = 341.23 Da; found: 342.23 Da $[\text{M}+\text{H}]^+$.

5-(Dimesitylboryl) benzene-1,3-diamine (3): Compound 3 was prepared following a procedure similar to that used for compound 2. The quantities involved and characterization data are as follows. 5-bromobenzene-1,3-diamine (2 g, 10.69 mmol), *n*-BuLi (1.6 M, 29.00 mL, 47.00 mmol) ClSiCH_3 (5.80 g, 53.45 mmol). 5-bromobenzene-*N, N, N, N*-tetrasilyl-1,3-diamine was distilled out (~ 150 °C) under reduced pressure, Yield: 95%; ^1H NMR (400 MHz, CDCl_3 , 25 °C): δ (ppm) 6.79 (d, $J = 1.6$ Hz, 2H), 6.38 – 6.37 (m, 1H), 0.06 (s, 36H). Step2:- 5-bromobenzene-*N, N, N, N*-tetrasilyl-1,3-diamine (2.00 g, 4.20 mmol), *n*-BuLi (2.90 mL, 4.60 mmol), Mes_2BF (1.30 g, 5.04 mmol). The crude product was purified by column chromatography over neutral alumina using a mixture of petroleum ether and ethyl acetate (80:20 ratios) as eluent to obtain the title compound as a pale brown solid. Yield: 80%. M.P.: ~ 167 -169 °C. ^1H NMR (400 MHz, CDCl_3 , 25 °C): δ (ppm) 6.80 (s, 4H), 6.29 (d, $J = 2$ Hz, 2H), 6.17 (t, $J = 2$ Hz, 2H), 3.35 (s, 4H), 2.31 (s, 6H), 2.04 (s, 12H). ^{13}C NMR (100 MHz, CDCl_3 , 25 °C): δ (ppm) 148.8, 147.3, 142.4, 141.3, 138.8, 128.4, 113.8, 106.0, 23.6, 21.6. ^{11}B NMR (376.5 MHz, CDCl_3 , 25 °C): δ (ppm) 73.7. ESI-MS (positive ion mode): Mcalc. for $\text{C}_{24}\text{H}_{29}\text{BN}_2$ = 357.2502 Da; found: 357.2505 Da $[\text{M}+\text{H}]^+$. (Note: 5-

bromobenzene-1,3-diamine was prepared from m-dinitrobenzene by following the reported procedure²²).

4-(Dimesitylboryl)-N,N,2,3,5,6-hexamethylbenzenamine (4): Sodium hydride (27 mg, 2.2 mmol) was added to THF (20 mL) solution of **1** (200 mg, 1 mmol) at 0 °C under stirring. After 30 minutes, Mel (69 µL, 2.2 mmol) was added drop wise to the reaction mixture at ~ < 0 °C. The reaction mixture was warmed to room temperature and the stirring was continued at room temperature. The progress of the reaction was monitored by TLC. After complete consumption of reactants, the reaction mixture was quenched with saturated aqueous NH₄Cl solution. The organic layer was extracted with ethyl acetate and dried over Na₂SO₄, and concentrated under reduced pressure. The crude product was purified by column chromatography over neutral alumina using a mixture of petroleum ether and ethyl acetate (97:3 ratio) as eluent to obtain the title compound as colourless solid. Yield: 75 %. M.P: ~ 144-146 °C. ¹H NMR (400 MHz, CDCl₃, 25 °C): δ (ppm) 6.71 (br s, 4H), 2.81 (s, 6H), 2.25 (s, 6H), 2.08 (s, 6H), 1.94 (s, 18H). ¹³C NMR (100 MHz, CDCl₃, 25 °C): δ (ppm) 150.7, 145.4, 145.0, 140.9, 140.8, 139.0, 136.4, 132.6, 128.8, 128.7, 43.1, 23.2, 22.8, 21.3, 20.3, 15.2. ¹¹B NMR (376.5 MHz, CDCl₃, 25 °C): δ (ppm) 75.9. ESI-MS (positive ion mode): Mcalc. for C₃₀H₄₀BN = 425.4563 Da; found: 426.3461 Da [M+H]⁺.

3-(Dimesitylboryl)-N,N-dimethylbenzenamine (5): Compound **5** was prepared following a procedure similar to that used for compound **4**. The quantities involved and characterization data are as follows. Compound **2** (200 mg, 1 mmol), sodium hydride (31 mg, 2.2 mmol), Mel (80 µL, 2.2 mmol). The crude product was purified by column chromatography over neutral alumina using petroleum ether as eluent to obtain the title compound as a pale green solid. Yield: 83 %. M.P: ~ 141-143 °C. ¹H NMR (400 MHz, CDCl₃, 25 °C): δ (ppm) 7.23-7.20 (m, 1H), 6.93 (br s, 1H), 6.89-6.86 (m, 2H), 6.79 (br s, 4H), 2.85 (s, 6H), 2.29 (s, 6H), 2.01 (s, 12H). ¹³C NMR (100 MHz, CDCl₃, 25 °C): δ (ppm) 150.7, 142.4, 141.2, 138.7, 129.0, 128.4, 125.7, 121.0, 116.8, 41.3, 23.8, 21.7. ¹¹B NMR (376.5 MHz, CDCl₃, 25 °C): δ (ppm) 73.8. ESI-MS (positive ion mode): Mcalc. for C₂₆H₃₂BN = 369.3500 Da; found: 370.2756 Da [M+H]⁺.

5-(Dimesitylboryl)-N1,N1,N3,N3-tetramethylbenzene-1,3-diamine (6): Compound **6** was prepared following a procedure similar to that used for compound **4**, in two steps. The quantities involved and characterization data are as follows. Step 1: Compound **3** (200 mg, 1 mmol), sodium hydride (27 mg, 2.0 mmol), Mel (70 µL, 2.0 mmol). Step 2: sodium hydride (27 mg, 2.0 mmol), Mel (70 µL, 2.0 mmol). The crude product was purified by column chromatography over neutral alumina using a mixture of petroleum ether and ethyl acetate (95:5 ratios) as eluent to obtain the title compound as a yellow solid. Yield: 52 %. M.P: ~ 150-152 °C. ¹H NMR (400 MHz, CDCl₃, 25 °C): δ (ppm) 6.77 (s, 4H), 6.42-6.41 (m, 2H), 6.29 (br s, 1H), 2.85 (s, 12H), 2.29 (s, 6H), 2.03 (s, 12H). ¹³C NMR (100 MHz, CDCl₃, 25 °C): δ (ppm) 151.5, 147.0, 142.4, 140.9, 138.1, 128.0, 111.2, 102.0, 41.2, 23.5, 21.3. ¹¹B NMR (376.5 MHz, CDCl₃, 25 °C): δ (ppm) 73.4. ESI-MS (positive ion mode): Mcalc. for C₂₈H₃₇BN₂ = 412.4178 Da; found: 413.4256 Da [M+H]⁺.

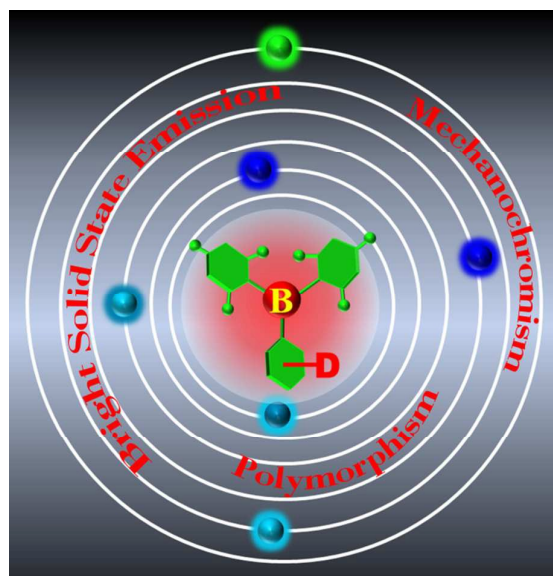
Acknowledgements

P. Thilagar and P. Sudhakar thanks Science and Engineering Research Board (SERB), New Delhi, India for financial support. K. K. Neena thanks CSIR New Delhi for research fellowship.

Notes and references

- 1 a) Y. Sagara and T. Kato, *Nat. Chem.*, 2009, **1**, 605-610; b) G. Cravotto, E. C. Gaudino and P. Cintas, *Chem. Soc. Rev.*, 2013, **42**, 7521-7534; c) M. Akita, *Organometallics*, 2011, **30**, 43-51; d) H. Sun, S. Liu, W. Lin, K. Y. Zhang, W. Lv, X. Huang, F. Huo, H. Yang, G. Jenkins, Q. Zhao and W. Huang, *Nat. Commun.*, 2014, **5**, 3601; e) T. Xia, L. Wang, Y. Qu, Y. Rui, J. Cao, Y. Hu, J. Yang, J. Wu and J. Xu, *J. Mater. Chem. C*, 2016, **4**, 5696-5701; f) L. Bai, P. Bose, Q. Gao, Y. Li, R. Ganguly and Y. Zhao, *J. Am. Chem. Soc.*, 2017, **139**, 436-441.
- 2 a) J. Lott, C. Ryan, B. Valle, J. R. Johnson, D. A. Schiraldi, J. Shan, K. D. Singer and C. Weder, *Adv. Mater.*, 2011, **23**, 2425-2429; b) D. R. T. Roberts and S. J. Holder, *J. Mater. Chem.*, 2011, **21**, 8256-8268; c) K. M. Wiggins, J. N. Brantley and C. W. Bielawski, *Chem. Soc. Rev.*, 2013, **42**, 7130-7147; d) Y. Fang, Y. Ni, S.-Y. Leo, B. Wang, V. Basile, C. Taylor and P. Jiang, *ACS Appl. Mater. Interfaces*, 2015, **7**, 23650-23659; e) Y. Jiang, G. Li, W. Che, Y. Liu, B. Xu, G. Shan, D. Zhu, Z. Su and M. R. Bryce, *Chem. Commun.*, 2017, **53**, 3022-3025; f) F. Xu, T. Nishida, K. Shinohara, L. Peng, M. Takezaki, T. Kamada, H. Akashi, H. Nakamura, K. Sugiyama, K. Ohta, A. Orita and J. Otera, *Organometallics*, 2017, **36**, 556-563.
- 3 a) J. Luo, L.-Y. Li, Y. Song and J. Pei, *Chem. Eur. J.*, 2011, **17**, 10515-10519; b) K. Ariga, T. Mori and J. P. Hill, *Adv. Mater.*, 2012, **24**, 158-176; c) Z. Chi, X. Zhang, B. Xu, X. Zhou, C. Ma, Y. Zhang, S. Liu and J. Xu, *Chem. Soc. Rev.*, 2012, **41**, 3878-3896; d) S. Mukherjee and P. Thilagar, *J. Mater. Chem. C*, 2016, **4**, 2647-2662; e) J. Wu, Y. Cheng, J. Lan, D. Wu, S. Qian, L. Yan, Z. He, X. Li, K. Wang, B. Zou and J. You, *J. Am. Chem. Soc.*, 2016, **138**, 12803-12812.
- 4 a) M. S. Kwon, J. Gierschner, S.-J. Yoon and S. Y. Park, *Adv. Mater.*, 2012, **24**, 5487-5492; b) Y. Dong, B. Xu, J. Zhang, X. Tan, L. Wang, J. Chen, H. Lv, S. Wen, B. Li, L. Ye, B. Zou and W. Tian, *Angew. Chem. Int. Ed.*, 2012, **51**, 10782-10785; c) Z.-H. Guo, Z.-X. Jin, J.-Y. Wang and J. Pei, *Chem. Commun.*, 2014, **50**, 6088-6090; d) Y. Sagara, S. Yamane, M. Mitani, C. Weder and T. Kato, *Adv. Mater.*, 2016, **28**, 1073-1095; e) L. Wang, K. Wang, B. Zou, K. Ye, H. Zhang and Y. Wang, *Adv. Mater.*, 2015, **27**, 2918-2922.
- 5 a) T. Mutai, H. Satou and K. Araki, *Nat. Mater.*, 2005, **4**, 685-687; b) Z. Zhang, B. Xu, J. Su, L. Shen, Y. Xie and H. Tian, *Angew. Chem. Int. Ed.*, 2011, **50**, 11654-11657; c) C. Yuan, S. Saito, C. Camacho, S. Irle, I. Hisaki and S. Yamaguchi, *J. Am. Chem. Soc.*, 2013, **135**, 8842-8845; d) B. Chen, G. Yu, X. Li, Y. Ding, C. Wang, Z. Liu and Y. Xie, *J. Mater. Chem. C*, 2013, **1**, 7409-7417; e) S. Yagai, T. Seki, H. Aonuma, K. Kawaguchi, T. Karatsu, T. Okura, A. Sakon, H. Uekusa and H. Ito, *Chem. Mater.*, 2016, **28**, 234-241; f) T. Wang, N. Zhang, J. Dai, Z. Li, W. Bai and R. Bai, *ACS Appl. Mater. Interfaces*, 2017, **9**, 11874-11881; g) X. Wei, L. Bu, X. Li, H. Ågren and Y. Xie, *Dyes Pigm.*, 2017, **136**, 480-487.
- 6 a) S. Varghese and S. Das, *J. Phys. Chem. Lett.*, 2011, **2**, 863-873; b) R. H. Pawle, T. E. Haas, P. Muller and S. W. Thomas Iii, *Chem. Sci.*, 2014, **5**, 4184-4188; c) R. Li, S. Xiao, Y. Li, Q. Lin, R. Zhang, J. Zhao, C. Yang, K. Zou, D. Li and T. Yi, *Chem. Sci.*, 2014, **5**, 3922-3928; d) J. Wu, J. Tang, H. Wang, Q. Qi, X. Fang, Y. Liu, S. Xu, S. X.-A. Zhang, H. Zhang and W. Xu, *J. Phys. Chem. A*, 2015, **119**, 9218-9224; e) M. Tanioka, S. Kamino, A. Muranaka, Y. Ooyama, H. Ota, Y. Shirasaki, J. Horigome, M. Ueda, M. Uchiyama, D. Sawada and S. Enomoto, *J. Am.*

- Chem. Soc.*, 2015, **137**, 6436-6439; f) K. K. Neena, P. Sudhakar, K. Dipak and P. Thilagar, *Chem. Commun.*, 2017, **53**, 3641-3644.
- 7 a) C. S. Jib, K. Junpei, N. Yoshinobu, A. Tatsuo and K. Takaki, *Chem. Lett.*, 2012, **41**, 65-67; b) Z. Ma, M. Teng, Z. Wang, S. Yang and X. Jia, *Angew. Chem. Int. Ed.*, 2013, **52**, 12268-12272; c) Q. Qi, J. Zhang, B. Xu, B. Li, S. X.-A. Zhang and W. Tian, *J. Phys. Chem. C*, 2013, **117**, 24997-25003; d) H. Yuan, K. Wang, K. Yang, B. Liu and B. Zou, *J. Phys. Chem. Lett.*, 2014, **5**, 2968-2973; e) H.-J. Kim, D. R. Whang, J. Gierschner, C. H. Lee and S. Y. Park, *Angew. Chem. Int. Ed.*, 2015, **54**, 4330-4333.
- 8 a) Y. Sagara, T. Mutai, I. Yoshikawa and K. Araki, *J. Am. Chem. Soc.*, 2007, **129**, 1520-1521; b) M. Sase, S. Yamaguchi, Y. Sagara, I. Yoshikawa, T. Mutai and K. Araki, *J. Mater. Chem.*, 2011, **21**, 8347-8354; c) K. Nagura, S. Saito, H. Yusa, H. Yamawaki, H. Fujihisa, H. Sato, Y. Shimoikeda and S. Yamaguchi, *J. Am. Chem. Soc.*, 2013, **135**, 10322-10325; d) T. Han, Y. Zhang, X. Feng, Z. Lin, B. Tong, J. Shi, J. Zhi and Y. Dong, *Chem. Commun.*, 2013, **49**, 7049-7051.
- 9 a) Y. Sagara and T. Kato, *Angew. Chem. Int. Ed.*, 2008, **47**, 5175-5178; b) Y. Sagara, S. Yamane, T. Mutai, K. Araki and T. Kato, *Adv. Funct. Mater.*, 2009, **19**, 1869-1875; c) S. Yamane, Y. Sagara, T. Mutai, K. Araki and T. Kato, *J. Mater. Chem. C*, 2013, **1**, 2648-2656; d) K. Goossens, K. Lava, C. W. Bielawski and K. Binnemans, *Chem. Rev.*, 2016, **116**, 4643-4807.
- 10 a) J. R. Lakowicz, *Principles of Fluorescence Spectroscopy*; Plenum Press: New York, 1999.
- 11 a) J. Wang, J. Mei, R. Hu, J. Z. Sun, A. Qin and B. Z. Tang, *J. Am. Chem. Soc.*, 2012, **134**, 9956-9966; b) X. Y. Shen, Y. J. Wang, E. Zhao, W. Z. Yuan, Y. Liu, P. Lu, A. Qin, Y. Ma, J. Z. Sun and B. Z. Tang, *J. Phys. Chem. C*, 2013, **117**, 7334-7347; c) G. Zhang, J. Sun, P. Xue, Z. Zhang, P. Gong, J. Peng and R. Lu, *J. Mater. Chem. C*, 2015, **3**, 2925-2932; d) Y. Q. Dong, J. W. Y. Lam and B. Z. Tang, *J. Phys. Chem. Lett.*, 2015, **6**, 3429-3436; e) K. K. Neena and P. Thilagar, *J. Mater. Chem. C*, 2016, **4**, 11465-11473.
- 12 a) C. D. Entwistle and T. B. Marder, *Angew. Chem. Int. Ed.*, 2002, **41**, 2927-2931; b) N. Matsumi and Y. Chujo, *Polym. J.*, 2007, **40**, 77-89; c) Z. M. Hudson and S. Wang, *Acc. Chem. Res.*, 2009, **42**, 1584-1596; d) C. R. Wade, A. E. J. Broomsgrove, S. Aldridge and F. P. Gabbaï, *Chem. Rev.*, 2010, **110**, 3958-3984; e) Y. Ren and F. Jakle, *Dalton Trans.*, 2016, **45**, 13996-14007; f) L. Ji, S. Griesbeck and T. B. Marder, *Chem. Sci.*, 2017, **8**, 846-863.
- 13 a) M. Elbing and G. C. Bazan, *Angew. Chem. Int. Ed.*, 2008, **47**, 834-838; b) A. Proñ, G. Zhou, H. Norouzi-Arasi, M. Baumgarten and K. Müllen, *Org. Lett.*, 2009, **11**, 3550-3553; c) E. Sakuda, Y. Ando, A. Ito and N. Kitamura, *J. Phys. Chem. A*, 2010, **114**, 9144-9150; d) Y. Kim, H.-S. Huh, M. H. Lee, I. L. Lenov, H. Zhao and F. P. Gabbaï, *Chem. Eur. J.*, 2011, **17**, 2057-2062; e) J. Yoshino, Y. Nakamura, S. Kunitomo, N. Hayashi and H. Higuchi, *Tetrahedron Lett.*, 2013, **54**, 2817-2820; f) Z. Zhang, R. M. Edkins, J. Nitsch, K. Fucke, A. Steffen, L. E. Longobardi, D. W. Stephan, C. Lambert and T. B. Marder, *Chem. Sci.*, 2015, **6**, 308-321; g) K. Suzuki, S. Kubo, K. Shizu, T. Fukushima, A. Wakamiya, Y. Murata, C. Adachi and H. Kaji, *Angew. Chem. Int. Ed.*, 2015, **54**, 15231-15235.
- 14 a) S. Yamaguchi, S. Akiyama and K. Tamao, *J. Am. Chem. Soc.*, 2000, **122**, 6335-6336; b) H. Ito, T. Abe and K. Saigo, *Angew. Chem. Int. Ed.*, 2011, **50**, 7144-7147; c) M.-G. Ren, M. Mao and Q.-H. Song, *Chem. Commun.*, 2012, **48**, 2970-2972; d) X. Liu, S. Li, J. Feng, Y. Li and G. Yang, *Chem. Commun.*, 2014, **50**, 2778-2780; e) P. Chen, X. Yin, N. Baser-Kirazli and F. Jäkle, *Angew. Chem. Int. Ed.*, 2015, **54**, 10768-10772; f) V. M. Hertz, M. Bolte, H.-W. Lerner and M. Wagner, *Angew. Chem. Int. Ed.*, 2015, **54**, 8800-8804; g) C. Wang, Q.-W. Xu, W.-N. Zhang, Q. Peng and C.-H. Zhao, *J. Org. Chem.*, 2015, **80**, 10914-10924; h) T. Hatakeyama, K. Shiren, K. Nakajima, S. Nomura, S. Nakatsuka, K. Kinoshita, J. Ni, Y. Ono and T. Ikuta, *Adv. Mater.*, 2016, **28**, 2777-2781.
- 15 a) P. Sudhakar, S. Mukherjee and P. Thilagar, *Organometallics*, 2013, **32**, 3129-3133; b) C. A. Swamy P. S. Mukherjee and P. Thilagar, *Chem. Commun.*, 2013, **49**, 993-995; c) S. K. Sarkar, G. R. Kumar and P. Thilagar, *Chem. Commun.*, 2016, **52**, 4175-4178.
- 16 a) B. Babb and P. J. Griddale, Canadian Patent CA 912019, 1972; b) J. C. Doty, B. Babb, P. J. Griddale, M. Glogowski and J. L. R. Williams, *J. Organomet. Chem.*, 1972, **38**, 229-236; c) M. E. Glogowski, P. J. Griddale, J. L. R. Williams and T. H. Regan, *J. Organomet. Chem.*, 1973, **54**, 51-60; d) M. E. Glogowski and J. L. R. Williams, *J. Organomet. Chem.*, 1981, **216**, 1-8; e) M. E. Glogowski and J. L. R. Williams, *J. Organomet. Chem.*, 1981, **218**, 137-146; f) Z. M. Hudson, C. Sun, M. G. Helander, Y.-L. Chang, Z.-H. Lu and S. Wang, *J. Am. Chem. Soc.*, 2012, **134**, 13930-13933.
- 17 S. Das, V. L. Alexeev, A. C. Sharma, S. J. Geib and S. A. Asher, *Tetrahedron Lett.*, 2003, **44**, 7719-7722.
- 18 a) L. Liu, T. Wen, W.-Q. Fu, M. Liu, S. Chen and J. Zhang, *CrystEngComm*, 2016, **18**, 218-221; b) Y. Wang, I. Zhang, B. Yu, X. Fang, X. Su, Y.-M. Zhang, T. Zhang, B. Yang, M. Li and S. X.-A. Zhang, *J. Mater. Chem. C*, 2015, **3**, 12328-12334; c) C. Dou, L. Han, S. Zhao, H. Zhang and Y. Wang, *J. Phys. Chem. Lett.*, 2011, **2**, 666-670.
- 19 a) N. Mataga, Y. Kaifu and M. Koizumi, *Bull. Chem. Soc. Jpn.*, 1956, **29**, 465-470; b) V. E. Lippert, *Z. Elektrochem.*, 1957, **61**, 962-975; c) W. Baumann, H. Bischof, J. C. Fröhling, C. Brittinger, W. Rettig and K. Rotkiewicz, *Journal of Photochemistry and Photobiology A: Chemistry*, 1992, **64**, 49-72.
- 20 a) SAINT-NT, Version 6.04; Bruker AXS: Madison, WI, 2001; b) SHELXTL-NT, Version 6.10; Bruker AXS: Madison, WI, 2000.
- 21 a) A. D. Becke, *J. Chem. Phys.* 1993, **98**, 5648; b) M. J. Frisch, G. W. Trucks, H. B. Schlegel, G. E. Scuseria, M. A. Robb, J. R. Cheeseman, G. Scalmani, V. Barone, B. Mennucci, G. A. Petersson, H. Nakatsuji, M. Caricato, X. Li, H. P. Hratchian, A. F. Izmaylov, J. Bloino, G. Zheng, J. L. Sonnenberg, M. Hada, M. Ehara, K. Toyota, R. Fukuda, J. Hasegawa, M. Ishida, T. Nakajima, Y. Honda, O. Kitao, H. Nakai, T. Vreven, J. A. Montgomery, Jr., J. E. Peralta, F. Ogliaro, M. Bearpark, J. J. Heyd, E. Brothers, K. N. Kudin, V. N. Staroverov, R. Kobayashi, J. Normand, K. Raghavachari, A. Rendell, J. C. Burant, S. S. Iyengar, J. Tomasi, M. Cossi, N. Rega, J. M. Millam, M. Klene, J. E. Knox, J. B. Cross, V. Bakken, C. Adamo, J. Jaramillo, R. Gomperts, R. E. Stratmann, O. Yazyev, A. J. Austin, R. Cammi, C. Pomelli, J. W. Ochterski, R. L. Martin, K. Morokuma, V. G. Zakrzewski, G. A. Voth, P. Salvador, J. J. Dannenberg, S. Dapprich, A. D. Daniels, O. Farkas, J. B. Foresman, J. V. Ortiz, J. Cioslowski and D. J. Fox, Gaussian 09, Revision A.02, Gaussian, Inc., Wallingford, CT, 2009; c) A. D. Becke, *Phys. Rev. A* 1988, **38**, 3098; d) C. Lee, W. Yang and R. G. Parr, *Phys. Rev. B* 1988, **37**, 785.
- 22 a) K. Rajesh, M. Somasundaram, R. Saiganesh and K. K. Balasubramanian, *J. Org. Chem.*, 2007, **72**, 5867-5869. b) US Pat., WO2011/75515 A1, 2011.



Bright tunable solid state emission, intriguing mechanochromism and polymorphism dependent optical features of a series of borylated aryl amines were demonstrated.